Structural Engineering and Mechanics, Vol. 42, No. 6 (2012) 815-829
DOI: http://dx.doi.org/10.12989/sem.2012.42.6.815

Integrated fire dynamic and thermomechanical modeling of a bridge under fire

Joonho Choi[1,3a], Rami Haj-Ali[1,2b] and Hee Sun Kim*[4]

[1]School of Civil and Environmental Engineering, Georgia Institute of Technology, Atlanta, GA 30332-0355, USA
[2]School of Mechanical Engineering, Tel-Aviv University, Ramat Aviv, Israel
[3]Engineering Department, O-Won General Construction & Develop Cooperation, Seoul, South Korea
[4]Architectural Engineering Department, Ewha Womans University, Seoul, South Korea

(Received August 5, 2011, Revised April 25, 2012, Accepted May 1, 2012)

Abstract. This paper proposes a nonlinear computational modeling approach for the behaviors of structural systems subjected to fire. The proposed modeling approach consists of fire dynamics analysis, nonlinear transient-heat transfer analysis for predicting thermal distributions, and thermomechanical analysis for structural behaviors. For concretes, transient heat formulations are written considering temperature dependent heat conduction and specific heat capacity and included within the thermomechanical analyses. Also, temperature dependent stress-strain behaviors including compression hardening and tension softening effects are implemented within the analyses. The proposed modeling technique for transient heat and thermomechanical analyses is first validated with experimental data of reinforced concrete (RC) beams subjected to high temperatures, and then applied to a bridge model. The bridge model is generated to simulate the fire incident occurred by a gas truck on April 29, 2007 in Oakland California, USA. From the simulation, not only temperature distributions and deformations of the bridge can be found, but critical locations and time frame where collapse occurs can be predicted. The analytical results from the simulation are qualitatively compared with the real incident and show good agreements.

Keywords: fire; thermomechanical behavior; transient-heat analysis; bridge; fire dynamics simulator; finite element analysis

1. Introduction

Concrete at elevated temperatures can drastically change their effective mechanical and thermal properties. The increase of temperature can cause phase change in concrete materials during heating, which affects the overall transient heat conduction and thus the mechanical response within the structural member. Harmathy (1983, 1988) reported experimental results for the temperature-dependent thermomechanical material properties, such as effective specific heat (thermal capacity),

*Corresponding author, Professor, E-mail: hskim3@ewha.ac.kr
[a]Deputy Department Head
[b]Professor

thermal conductivity, mass change rate, and thermal expansion, of different concrete materials. As for the steel, Qutinen and Makelainen (2004) performed small-scale tensile tests using the transient state tensile method to study the mechanical properties of structural steels under high temperatures. In their study, accurate temperature dependent mechanical properties, such as yield strength, elastic modulus, and thermal elongation of steel were provided. Two grades of steel were tested at elevated temperatures. Chen *et al.* (2006) suggested reduction factors of the yield strength and elastic modulus of high and mild strength steels at elevated temperatures. They compared the experimentally obtained reduction factors with the ones provided from four design codes: American, Australian, British, and European standards, and concluded that the reduction factors for the yield strengths provided from the four design codes were conservative compared to the test results up to 1000^{o}C. The elastic modulus of high-strength steel from the American, Australian, and European standards were also conservative compared to the steady-state tests but unconservative compared to the transient-state tests.

Although relatively limited studies have been reported on the thermal and mechanical behaviors of bridges subjected to localized fire and severe conditions, the effect of thermal environmental conditions on the behaviors of bridges has been investigated by Moorty and Roeder (1992), Branco and Mendes (1993), Silveira *et al.* (2000). The one dimensional heat transfer analysis and thermoelastic analysis were used to find out behavior of bridges under thermal environmental conditions by Moorty and Roeder (1992). They suggested additional guidelines and recommendations to accurately predict thermal movements and the placement of bearings and expansion joints. Branco and Mendes (1993) also proposed numerical method using the Fourier heat-transfer equation to obtain the nonlinear temperature distributions for the concrete bridges using finite element (FE) method, considering geometry of the cross section, the thermal material properties concrete, and the location of the bridge were also taken into account in the model. Silveira *et al.* (2000) proposed a numerical method to get the temperature distributions of the concrete bridge considering climatic conditions. The temperature distributions were calculated using two-dimensional Fourier heat-transfer equation which considered the bridge cross section, the thermal material properties of concrete and asphalt, and climatic conditions.

Analytical methods have been developed to predict bridge behaviors subjected to fire and applied to real fire cases occurred at bridges, such as S. Lourenco bridge, Vasco da Gama Bridge, and Vivegnis Bridge. Neves *et al.* (1997) analyzed the effects of wood formwork fire accidents during the bridge construction based on the fire accident occurred at the S. Lourenco bridge. The finite element method was used to perform thermal analysis and to support decision whether repair or demolition of the damaged bridge was needed. Mendes *et al.* (2000) developed a 2D partial numerical bridge deck model and applied for fire accident occurred at Vasco da Gama Bridge. They predicted temperature distributions of the cross section at 4 different times (30, 60, 90, and 120 min) for different fire conditions. Dotreppe *et al.* (2006) performed numerical analysis using SAFIR computer code developed at the University of Liege for the Vivegnis Bridge collapse by an accident with severe localized fire occurred at one of the bridge foot due to a gas pipe explosion. In the dynamic structural analysis, 3D beam elements were generated for main girders, cross girders, concrete slab, arches, and bracings and truss for the suspenders, and high temperatures were applied to one of the foot of abutment area based on the hydrocarbon temperature-time curve of Eurocode 1, part 1-2 (1995). The failure time and mode showed good agreement with optical observations of the bridge collapse.

These analytical studies were performed using linear 2D or simple 3D element model and only focused on one specific part such as the heat transfer or the thermomechanical analysis. The calculated temperature distributions for the bridge were also not obtained from fire simulation or real fire temperature data and the structural behaviors were predicted by temperature distributions from literature, not from analytical model.

Besides the investigations about concrete deck bridges, the analytical studies for the fiber reinforced polymer (FRP) bridge deck system under thermal loadings were also reported by Alnahhal *et al*. (2006, 2007), and Keller *et al*. (2006). In this paper, a combined 3D fire dynamic, thermal, and structural analysis framework is proposed where nonlinear and damage material behavior as well as fire scenario is integrated to predict structural behaviors of bridge including damage evaluation during and after the fire incident. Toward this goal, a transient heat finite element analysis is proposed with nonlinear material parameters as a function of temperature and validated with the existing experimental data of RC beams subjected to fire. New software in the form of user subroutines is written, in part, to model internal chemical reaction expressed by the change of the effective specific heat, conductivity, and coefficient of thermal expansion in materials as a function of temperature. The proposed integrated fire dynamic and thermomechanical modeling approach is applied to simulate fire incident occurred at a bridge in Oakland California, USA, in 2007.

2. Modeling approaches

2.1 Modeling framework

In this modeling framework, analysis of structures under combined mechanical and fire loads are carried out using the Fire Dynamics Simulator (FDS) and ABAQUS FE codes. The FDS is first used to solve for the temperature or heat flux on the surfaces as a function of time. A simple heat release rate as a function of time is used to represent the energy released from the surface of the fire source in the model. The solutions for the surface heat and temperature of the steel beams and columns obtained from the fire model are approximated using a fourth-order polynomial in time with coefficients that are spatially dependent. The temperature distributions within the steel beams are assumed to be linear as a function of the upper and lower surface temperatures. However, the 3D temperature distribution for the concrete slabs is more complicated and is determined from a separate heat transfer analysis using the surface heat flux polynomial approximations as boundary conditions. The nonlinear structural analysis is sequentially carried out once the temperature distributions are obtained as a function of time within all points in the structure (Choi *et al*. 2010).

Fig. 1 shows a general framework for the analysis of structures under combined fire and mechanical loading. The proposed approach can be divided into three simulation parts. The first part is the fire simulation where the fire model is utilized. The fire model generates a solution of several state variables, such as pressure, temperature, heat, velocity vector. However, our framework is interested in the heat and temperature solution part that are related to the structure performance and response. The temperature and heat flux of the interior structural surfaces profiles are used and applied to subsequent simulation parts. The second part is the heat transfer analysis. The objective of this part is to compute the temperature profiles for the different structural components, beams, columns, and especially the concrete slabs through their thickness using the heat flux or surface temperature results from the fire model. The third part is the nonlinear 3D structural analysis. The temperature profiles in this modeling stage is known and imposed spatially as a function of time.

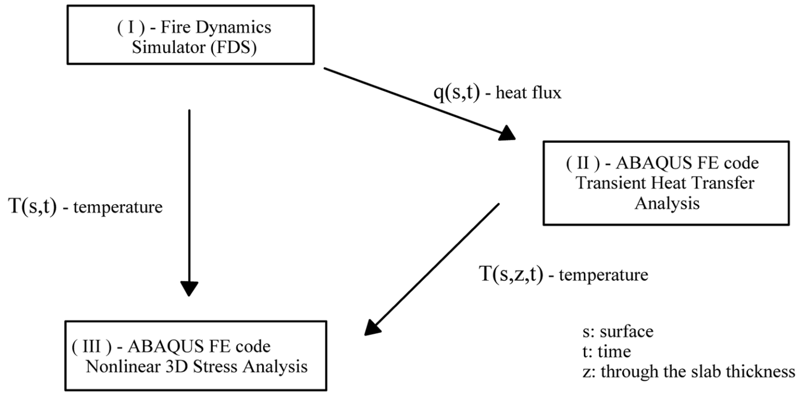

Fig. 1 Proposed sequential fire-heat-structural analysis framework

2.2 Transient heat formulation

Transient heat formulations are written considering temperature dependent thermal material properties and implemented within heat transfer analysis. The energy conservation principle can be stated as the internal heat energy rate stored inside a solid is equal to the balance of externally supplied and emitted heat energy fluxes transmitted on the surface of the solid. This is simply expressed as

$$\dot{Q}_{in} = \dot{Q}_{out} \tag{1}$$

The internal volumetric heat energy rate produced inside the solid, $\dot{Q}_{in}$, can be rewritten as

$$\dot{Q}_{in} = \int_V \frac{\partial}{\partial t}(\rho Q_{in})dV = \int_V (\rho \dot{Q}_{in} + \dot{\rho} Q_{in})dV \tag{2}$$

where Q_{in} is the internal heat energy density per unit mass, and $\dot{\rho}$ is the density rate. The rate of the internal energy density can be rewritten using the derivative chain rule as

$$\frac{dQ_{in}}{dt} = \frac{dQ_{in}}{d\theta(x,t)}\frac{d\theta(x,t)}{dt} = C_p(\theta)\frac{d\theta(x,t)}{dt} \tag{3}$$

where $d\theta(x,t)$ is the current spatial temperature field, and x denotes the spatial location vector in 3D space. The rate of the internal energy density with respect to the temperature expresses the internal heat capacity absorption property of the material, known as the specific heat capacity (C_p). Substituting Eq. (3) into Eq. (2), and assuming a constant density, the rate of the internal energy density yields

$$\dot{Q}_{in} = \int_V \rho\frac{dQ_{in}}{dt}dV = \int_V \rho\frac{dQ_{in}}{d\theta(x,t)}\frac{d\theta(x,t)}{dt}dV = \int_V \rho C_p(\theta)\frac{d\theta(x,t)}{dt}dV \tag{4}$$

$$\dot{Q}_{out} = \int_s q_i \cdot n_i ds = \int_s \left(k(\theta)\frac{d\theta(x,t)}{dx_i}\right)\cdot n_i ds = \int_V \frac{d}{dx_i}\cdot\left(k(\theta)\frac{d\theta(x,t)}{dx_i}\right)dV \tag{5}$$

where q_i is the surface heat flux vector, and k is the thermal conductivity. Combining Eqs. (4) and (5), the partial differential (heat conduction) equation (PDE) can be developed as

$$\int_V \rho C_p(\theta)\frac{d\theta(x,t)}{dt}dV = \int_V \frac{d}{dx_i}\cdot\left(k(\theta)\frac{d\theta(x,t)}{dx_i}\right)dV \tag{6}$$

Since the volume is arbitrary, the Eq. (6) becomes

$$\rho C_p(\theta)\frac{d\theta(x,t)}{dt} = \frac{d}{dx_i}\cdot\left(k(\theta)\frac{d\theta(x,t)}{dx_i}\right) \tag{7}$$

Eq. (7) can be considered as a linear PDE, if ρ, C_p, k are constant and solved using classical numerical techniques, including the finite element (FE) method. In the case where the latter material properties are functions of temperature, the PDE is a nonlinear and a more complex numerical technique is required for general solutions, e.g. concrete under high temperatures. In this study, the ABAQUS general purpose FE code is used for both the nonlinear transient heat and the thermomechanical analyses. In the former case, the concrete temperature dependent specific heat capacity is included as an external code used to describe the material thermal behavior. This general code basically updates the internal thermal energy per unit mass at the end of the time increment. The temperature gradient of the internal energy is also required as well as the matrix form of the gradient spatial derivatives. Finally, the heat flux and its gradients are also required to complete the nonlinear heat transient analysis. In our code, we define the temperature-dependent heat capacity and conductivity as internal flux terms calculated as part of the total internal energy density.

Lower and upper bounds of effective specific heat and conductivity of concretes are identified based on Harmathy (1983, 1988) where several other reported results for different concretes are within these bounds depending on the aggregates, admixtures, and mix proportions.

The thermal energy from the known remote heat sources is applied into the surface of the structures through convection heat transfer. Therefore, a convection heat flux is applied as a boundary condition on the exposed surfaces. The applied convection heat flux is linearly related to the surface temperature differences through a convection coefficient (h) and described by

$$q_c = h(\theta - \theta_c) \tag{8}$$

where, the remote temperature, θ_∞, is the ambient temperature, and the range of h for air medium can vary from 2 W/m^2°C to 25 W/m^2°C.

2.3 Model validation

In order to validate the proposed modeling framework, experimental results of RC beams under fire are used. In the experiments, the RC beams are heated by ISO-834 heating curve shown in Fig. 2, and temperature distributions and the deformations are obtained during the tests. The dimension of the tested beams is 0.250.4 m in cross section and 5 m in span. Fig. 3 shows the detail of the cross section with reinforcements and three thermocouples placed at the mid-span section to obtain temperature data during fire tests. The 28-day compressive concrete strength is tested from cylindrical specimens and found to be 21.42 MPa. The fire test set up for the concrete beams is shown in Fig. 4. The detailed experimental works on RC beams can be found in Shin (2003).

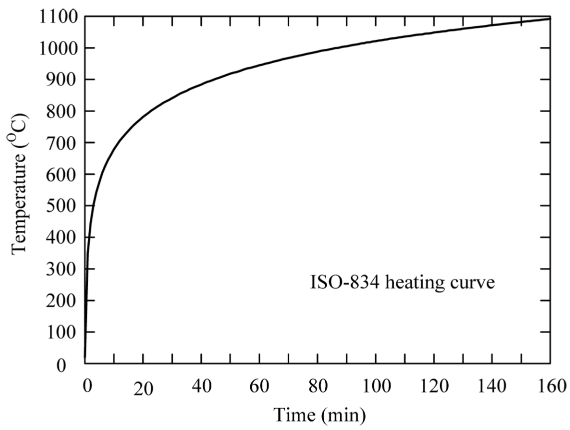

Fig. 2 ISO-834 time dependent heating curve

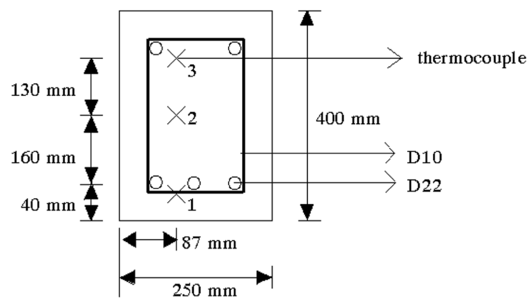

Fig. 3 Section of concrete beam

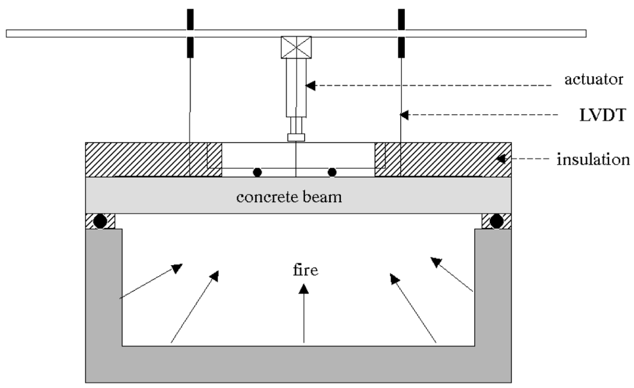

Fig. 4 Set-up for fire test on concrete beam

For the transient heat analysis, 8-noded 3D diffusive heat transfer elements are adopted and the mesh is refined to match the locations of thermocouples and reinforcements used in the experiments. The nodal temperatures obtained from the heat transfer analysis are used sequentially in the thermal stress analysis conducted while the beams are subject to constant load of 88.8 kN for

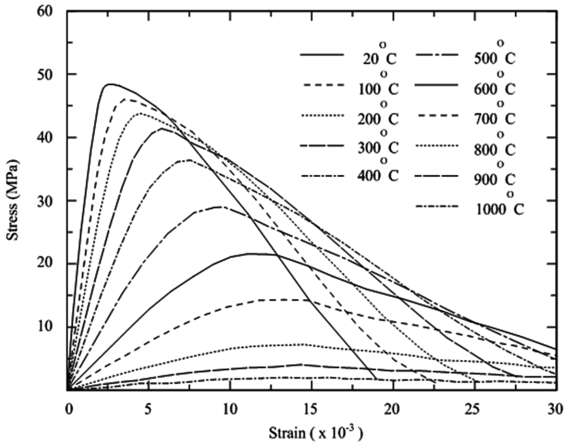

Fig. 5 Concrete compressive stress-strain curves at elevated temperatures (Adapted from Eurocode-2, ENV 1992-1-2:1995)

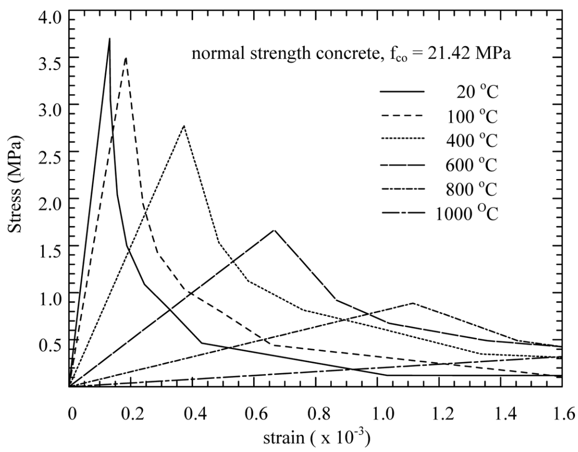

Fig. 6 Re-constructed concrete tensile stress-strain curves at elevated temperatures

RC beam as performed in the tests. In thermal stress analysis, 8-noded 3D displacement brick elements are used with the same mesh refinement and time steps as the previous heat transfer analysis. The thermal and mechanical material properties for concrete and their temperature dependent are obtained from the literatures, e.g., ACI report (1994) and Harmathy (1983, 1988). These include the effective specific heat, conductivity, coefficient of thermal expansion, degraded elasticity modulus, and compressive stress-strain relationships. Fig. 5 shows the concrete compressive stress-strain relations at different temperatures. The tensile stress-strain relations of concrete under high temperatures are assumed based on the room temperature experimental data performed by Gopalaratnam and Shah (1985). Fig. 6 illustrates the assumed tension stress-strain curves for RC at elevated temperatures using room temperature curves but scaled based on compressive relationship in Fig. 5.

For reinforcing bars, thermal and mechanical material properties of steel are used. Mechanical material behaviors of steel are temperature dependent as provided from Eurocode 3 (1995), while the effect of temperature of thermal material properties is ignored in this study.

Based on the parametric studies, a convection coefficient of 20 W/m^{2o}C and averaged bound of effective specific heat and thermal conductivity are applied to the heat transfer analysis of the RC beam. In the thermal stress analysis for RC materials, thermomechanical material properties, such as CTE and degradation ratio of elastic modulus are used based on the siliceous aggregate curves. Fig. 7 shows the nonlinear transient heat temperature solutions through the section of RC beam compared with experimental results measured at points 1, 2, and 3. Overall, the proposed model shows good agreement compared with the experimental results; however, the temperatures at point 2 and 3 obtained from the heat transfer analysis are higher than the experiments above the 75 minute time range. This can be explained by the moisture content of concrete beam. Large amount of moisture compared to a concrete structure members maybe present since the fire tests are conducted only three months after curing. The large amount of moisture inside the tested concrete beam is evaporated when the concrete is exposed to temperatures beyond 100°C, which delays the heat conduction.

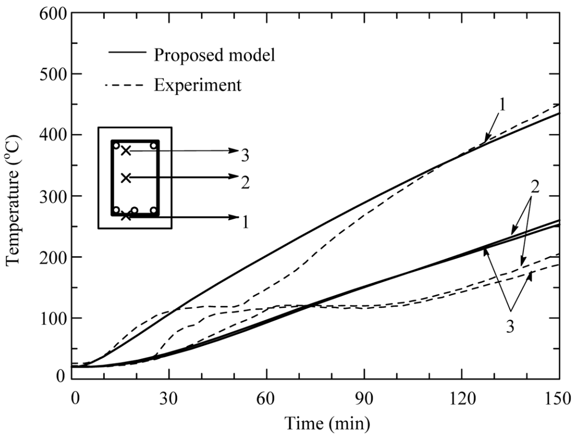

Fig. 7 Comparison between analytical and experimental results of temperature distributions over a cross section of RC beam

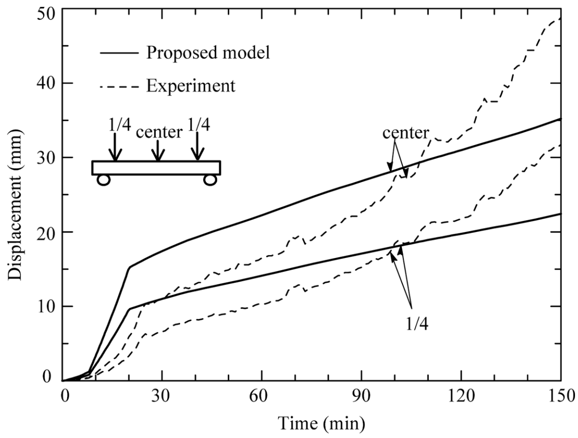

Fig. 8 Analytical and experimental results of deflections of RC beam under thermal and mechanical loading observed at center and 1/4 of beam span

Fig. 8 shows the deflections at the center and the 1/4 point of the beam-span obtained from the analytical model and experiments. As seen from the experimental results, the deflections increase rapidly after 90 minute of heating. The rapid increase of deflections can be attributed to the damage in concrete materials, especially softening due to cracking.

3. Model application to the Fuel-truck accident on I-880, California, USA

A highway bridge overpass in the East Bay's MacArthur Maze was collapsed on April 29, 2007. Figs. 9(a) and (b) indicate the collapsed highway bridge location. It was located at the eastbound connector to Interstate-580 overpass the southbound connector Interstate-80 to Interstate -880 in Oakland, California. The collapse was occurred by a fuel-truck accident. A gasoline truck crashed and burst into flames on the southbound connector I-80 to I-880 under the I-580 around 3:40 am near the San Francisco Bay Bridge. Because of the heat from the flames, two spans of the I-580

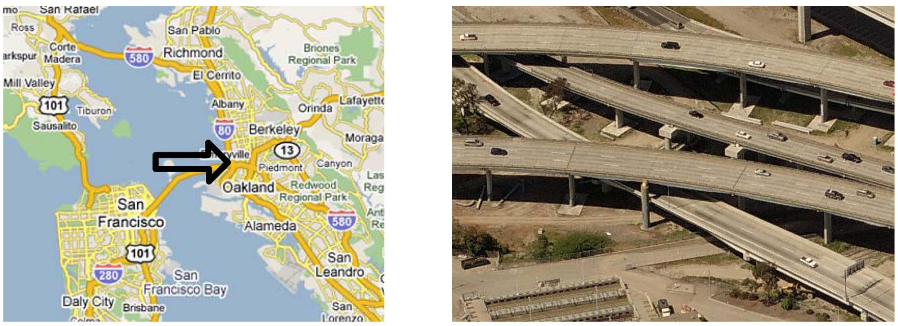

(a) Google maps (http://maps.google.com/) (b) Live Search maps (http://maps.live.com/)

Fig. 9 Oakland I-580 Bridge over I-880

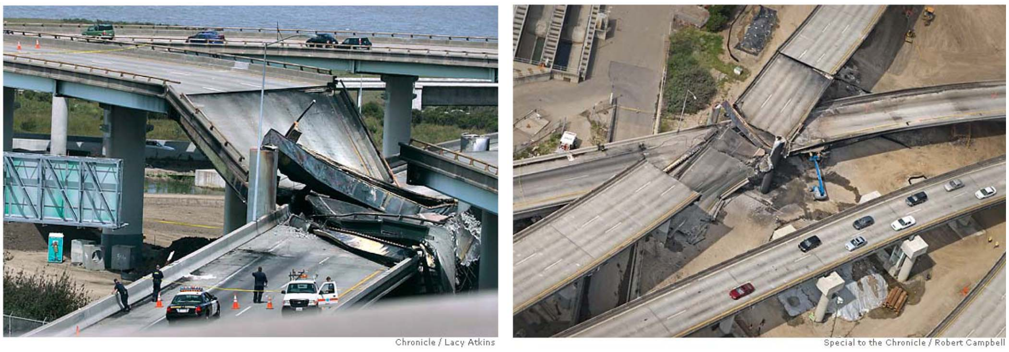

(a) Photo by Lacy Atkins (b) Photo by Robert Campbell

Fig. 10 The collapsed bridge (eastbound connector to I-580)

Bridge were collapsed around 4:00am, occurred 20 minute after the truck was crashed. Fig. 10 shows the bridge after it was fallen down with different views. A total of 8600 gallons of unleaded gasoline was spilled and burned, according to FOX news (2007). Two hundred eighty thousand commuters take the bridge into San Francisco every day. The bridge was re-opened on May 25, 2007 in the morning. Replacing steel girders and decks took 26 days.

4. Analytical results

4.1 Fire dynamics simulation model

Fire model is generated for the collapsed I-580 bridge including I-80/880 bridge where the gasoline truck was crashed. Fig. 11 shows the fire bridge model with overall and on the I-80/880 bridge deck view. The bridge geometry is approximated based on Google satellite maps because the exact bridge dimensions are not found in public. The assumed width and height of the bridge are as 14 and 10 meters respectively. The spilled gasoline from the crashed truck is shown in Fig. 11 as orange color objects. Ninety percent of the total spilled gasoline (8600 gallons) is on the I-80/880 bridge deck and other ten percent of gasoline is on the ground because we assume that most of the spilled gasoline is on the bridge but also some of it flowed to the ground. Heat release rate per unit

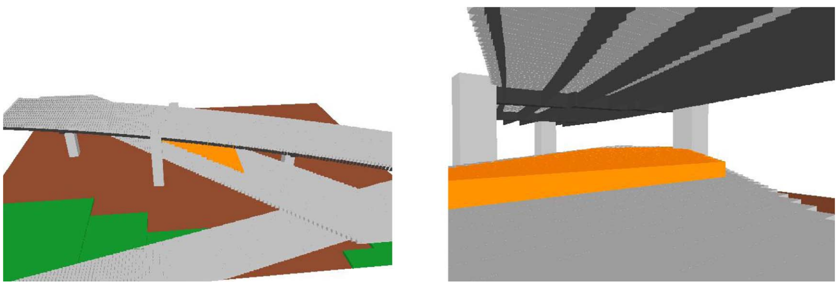

Fig. 11 Fire bridge model

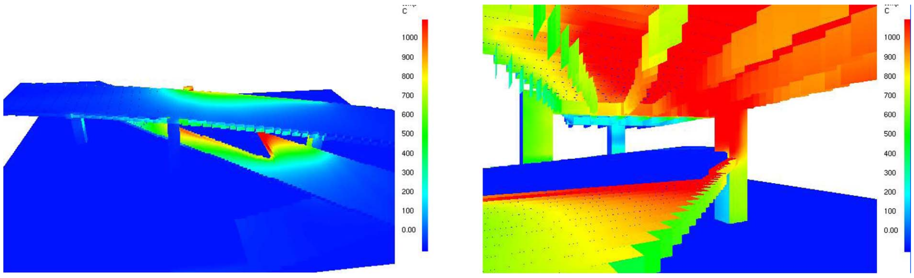

Fig. 12 Collapsed bridge fire model with temperature contour results

area for the fire source is assumed as 2500 kW/m^2 during 21 minutes. It is also assumed that the fire is ignited very quickly and then suddenly approached to steady-state phase. The concrete material is used for bridge decks and columns and steel is for bridge girders. The gray and black objects represent concrete and steel. Wind is also considered as 2.6 m/s NW (The weather underground, Inc. 2007) in the fire model.

Fig. 12 shows the surface temperature fire model results at the end of simulation when the time is at 21 minute after fire started. The temperatures above the spilled gasoline are around 1000^{o}C in the figures. The surface heat flux and temperature results from the fire simulation will be used in the nonlinear transient heat transfer and three dimensional thermal stress analyses.

4.2 Nonlinear transient heat analysis

A separate nonlinear heat transfer analysis for the Oakland Bridge was also performed to get the temperature profiles for the concrete deck. The nonlinear transient heat analysis was modeled using four-node quadrilateral shell elements and the concrete bridge deck was only considered in this model. The fire model heat flux results were applied as boundary conditions to the bottom surface of the deck while a room temperature was employed to the top surface. Fig. 13 presents the positions through the concrete deck where the temperatures are predicted and Fig. 14 shows the locations where FE predictions of temperatures and vertical displacements.

The temperatures for the steel girders and diaphragms obtained from fire model and applied to the 3D thermomechanical analysis are shown in Fig. 15 at four different locations. The location D3 is the place where the maximum temperature occurred. It reaches around 1200^{o}C at 20 minute. The 3D thermomechanical FE model for the Oakland Bridge consists of 3D beam elements (Timoshenko beam theory) used for the flange of the steel girders as seen in Fig. 16. In the model, four-node shell elements are used for the concrete deck, steel girders' web, and diaphragms. The

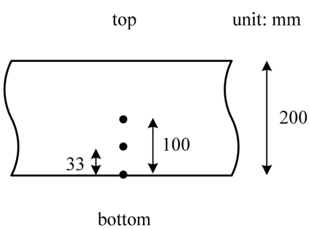

Fig. 13 Bridge deck FE model cross section

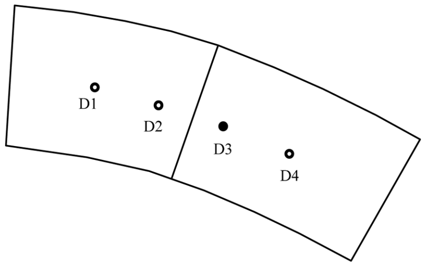

Fig. 14 Locations selected for plotting analytical results

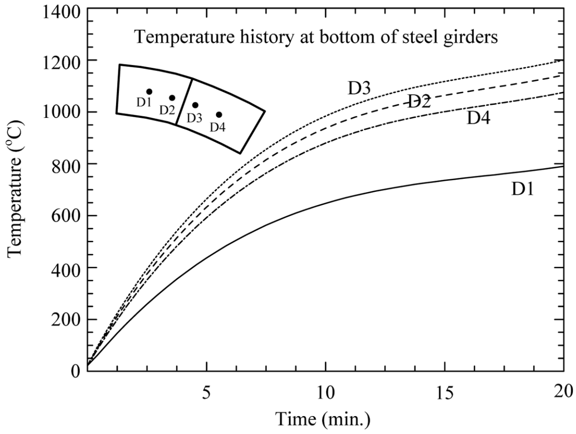

Fig. 15 The temperatures predicted from fire model and applied to thermomechanical analysis at selected locations

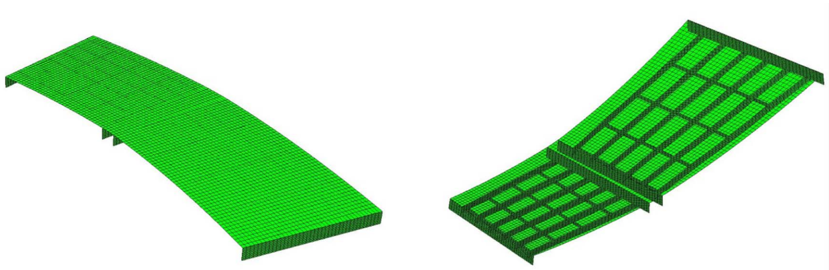

Fig. 16 Oakland Bridge FE model

heat transfer analysis provides the temperature histories for the concrete bridge deck. Two spans and six steel girders for each span are included in the FE model. Total fifty diaphragms are also considered. In addition, the concrete deck and steel girders are fully connected. Because the dimensions of the bridge are not known to public, several photos in the California Department of Transportation District 4 website are used to determine the geometries (California DOT 2007). For our FE model, thickness of the concrete deck set as 0.2 m. For other geometries, 1 m, 0.0254 m, 0.3 m, and 0.0381 m are employed for the steel girders' web height, web thickness, flange width, and flange thickness, respectively. Self weight of steel girders and concrete deck, parapets, and wearing surface are taken into account as a dead load. The 0.48 m width by 0.74 m height of

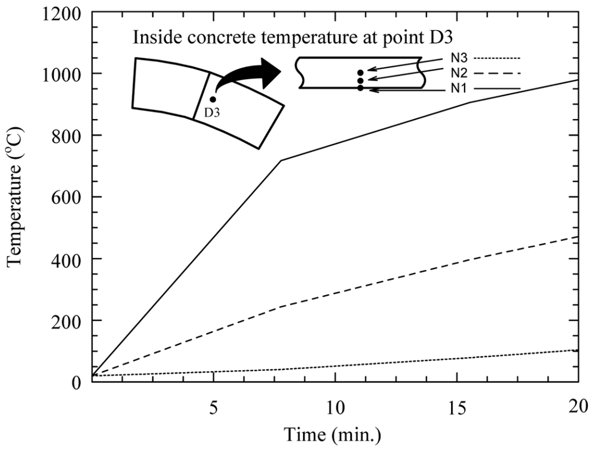

Fig. 17 Temperature prediction through the concrete deck using heat transfer analysis

parapets is assumed to be placed at the both ends of the highway bridge. Also, the wearing surface of 1200 N/m^2 is included in the dead load. The boundary conditions at the end of bridge spans are considered as simply supported. The concrete deck and the steel girders are fully connected in the model.

Nonlinear FE transient heat prediction temperature results for the concrete bridge deck at location D3 are shown in Fig. 17. The temperature at bottom and middle of the deck is shown using a solid line (N1) and dash line (N3) respectively. The temperature of the concrete bottom deck is increased rapidly until 7 minutes and then reached around 1000°C at 20 minute.

4.3 Thermomechanical analysis

The predicted vertical displacements from 3D thermomechanical analysis at four different locations are shown in Fig. 18 until the time reaches 20 min. Relatively large displacements are shown at the middle of the right span of the bridge (D4). Fig. 19 shows the bridge pictures of actual

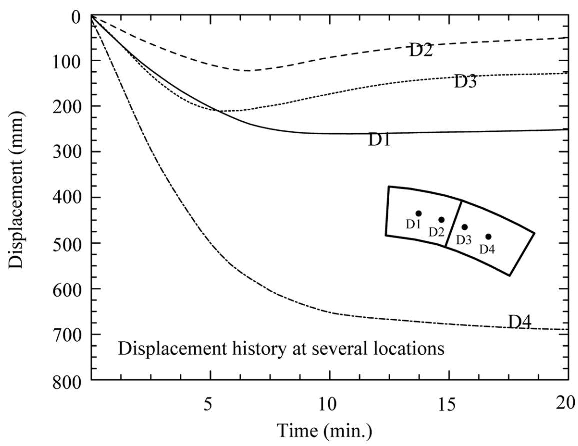

Fig. 18 Predicted displacements of the Oakland Bridge model at selected locations

<table>
<tr><td>An image captured from Public Broadcasting Service (PBS, 2007)</td><td></td></tr>
<tr><td>Results from Fire dynamic simulation model</td><td>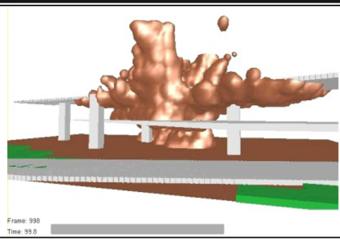</td></tr>
<tr><td>Temperature contour of FE structural model (°C)</td><td>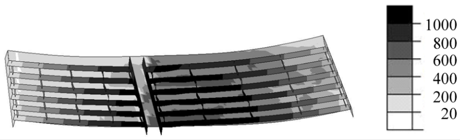
</td></tr>
<tr><td>Equivalent plastic strain contour of FE structural model (%)</td><td>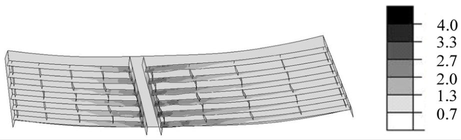
</td></tr>
<tr><td>Vertical displacement contour of FE structural model (m)</td><td>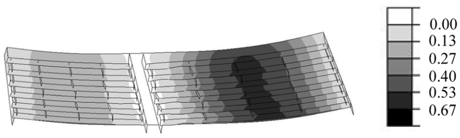
</td></tr>
</table>

Fig. 19 Predictions from the Oakland Bridge model compared to an image captured from actual video at 20 mins after the fire

video, fire model, and thermomechanical model at 20 min after the fire. An image captured from the actual video shows the bridge just before collapsed. Around that time, the right span of the bridge shows large deflections and the steel girders near the middle support area are also yielded. The bridge collapse is started at the middle support area of the right span in the actual happening. The reason why the FE model does not show the exact bridge collapse behavior is that the actual dimension and geometry of the bridge are not used in the model. However, the results using our proposed framework predict the overall behavior of the bridge under fire conditions.

5. Conclusions

An application of the integrated fire dynamics and thermomechanical framework is presented in this paper. The nonlinear transient heat analysis for concrete materials is carried using FE formulation. This study uses the ABAQUS implicit FE code with external user subroutines written to add the material properties dependent on the high magnitude of temperature. From the model validation, it is found that in order to properly simulate concrete thermal behavior, the effective specific heat and conductivity is temperature dependent and will change the nature of the heat conduction PDE. Once the thermal model is solved, a sequential coupling is performed by using the spatial temperature distribution in another thermomechanical FE structural modeling. The proposed analysis framework is applied to Oakland bridge collapse due to fire truck accident to predict thermomechanical behaviors of the various structures and evaluate the damage level under fire conditions. The application shows a possibility that the proposed analysis framework can be used to simulate not only the building structures but also to evaluate structural performance of various civil structures under fire conditions.

References

ACI Committee 216 (1994), "Guide for determining the fire endurance of concrete elements", *American Concrete Institute Committee Report*, 216R1-48.

Ahmed, G. and Hurst, J.P. (1999), "Modeling pore pressure, moisture, and temperature in high strength concrete columns exposed to fire", *Fire Technol.*, **35**, 232-262.

Alnahhal, W.I., Chiewanichakorn M., Aref, A.J. and Alampalli, S. (2006), "Temporal thermal behavior and damage simulations of FRP deck", *J. Bridge Eng.*, **11**(4), 452-464.

Alnahhal, W.I., Chiewanichakorn, M. and Aref, A.J. (2007), "Simulations of structural behaviour of fibre-reinforced polymer bridge deck under thermal effects", *Int. J. Mater. Product Technol.*, **28**(1-2), 122-140.

Branco, F.A. and Mendes, P.A. (1993), "Thermal actions for concrete bridge design", *J. Struct. Eng.*, **119**(8), 2313-2231.

California Interchange Collapses After Tanker Fire, FOX news Channel (2007), http://www.foxnews.com/story/0,2933,269118,00.html

Chen, J., Young, B. and Uy, B. (2006), "Behavior of high strength structural steel at elevated temperatures", *J. Struct. Eng.*, **132**, 1948-1954.

Cheng, F., Kodur, V.K.R. and Wang, T. (2004), "Stress-strain curves for high strength concrete at elevated temperature", *J. Mater. Civil Eng.*, **16**(1), 84-90.

Choi, J., Kim, H.S. and Haj-Ali, R.M. (2010), "Integrated fire dynamics and thermomechanical modeling framework for steel-concrete composite structures", *Steel Compos. Struct.,* **10**(2), 129-149.

Dotreppe, J.C., Majkut, S. and Franssen, J.M. (2006), "Failure of a tied-arch bridge submitted to a severe localized fire", *Struct. Extreme Events*, IABSE Symposium, 272-273.

Elghazouli, A.Y. and Izzuddin, B.A. (2000), "Response of idealised composite beam-slab systems under fire conditions", *J. Constr. Steel Res.*, **56**, 199-224.

Elghazouli, A.Y. and Izzuddin, B.A. (2004), "Realistic modeling of composite and reinforced concrete floor slabs under extreme loading. I: analytical method", *J. Struct. Eng.*, **130**(12), 1972-1984.

Elghazouli, A.Y., Izzuddin, B.A. and Richadson, A.J. (2000), "Numerical modeling of the structural fire behavior of composite buildings", *Fire Safety J.*, **35**, 279-297.

ENV (1995), "Eurocode 2: Design of concrete structures - Part 1-2: General rules - Structural fire design", 1992-1-2 European Pre-standard.

ENV (1995), "Eurocode 3: Design of Steel Structures - Part 1-2: Fire Resistance", 1993-1-2 European Pre-standard.

Gopalaratnam, V.S. and Shah, S.P. (1985), "Softening response of plain concrete in direct tension", *J. Am. Concrete Inst.*, **82**, 310-323.

Harmathy, T.Z. (1983), "Properties of building materials at elevated temperatures", DRP Paper No. 1080 of the Division of Building Research.

Harmathy, T.Z. (1988), "Properties of building materials in SFPE Handbook of fire protection engineering", Ed. DiNenno, P.J. *et. al*, Section 1, Chapter 26, 378-391.

History for Oakland, CA on Sunday, April 29 (2007), The weather underground, Inc. http://www.wunderground.

com/history/airport/KOAK/2007/4/29/DailyHistory.html

Keller, T., Tracy, C. and Hugi, E. (2006), "Fire endurance of loaded and liquid-cooled GFRP slabs for construction", *Compos. Part A-Appl. S.*, **37**(7), 1055-1067.

Kodur, V.K.R. and Sultan, M.A. (2003), "Effect of temperature on thermal properties of high-strength concrete", *J. Mater. Civil Eng.*, **15**(2), 101-107.

Marzouk, H. and Chen, Z.W. (1995), "Fracture energy and tension properties of high-strength concrete", *J. Mater. Civil Eng.*, **7**, 108-116.

Maze Damage & Repair Photographs, California Department of Transportation District 4 (2007), http://www.dot.ca.gov/dist4/mazedamage/mazephotos.htm

Mendes, P.A., Valente, J.C. and Branco, F.A. (2000), "Simulation of ship fire under Vasco da Gama Bridge", *ACI Struct. J.*, **97**(2), 285-290.

Moorty, S. and Roeder, C.W. (1992), "Temperature-dependent bridge movements", *J. Struct. Eng.*, **118**(4), 1090-1105.

Neves, I.C., Branco, F.A. and Valente, J.C. (1997), "Effects of formwork fires in bridge construction" *Concrete Int.*, **19**(3), 41-46.

Outinen, J. and Makelainen, P. (2004), "Mechanical properties of structural steel at elevated temperatures and after cooling down", *Fire Mater.*, **28**, 237-251.

Shin, M., Kim, H.S. and Shin, Y.S. (2003), "Structural behavior of flexural member with normal & high strength concrete under high temperature", *Proceedings of Korea Institute for Structural Maintenance Inspection*, **7**(2), 157-160.

Silveira, A.P., Branco, F.A. and Castanheta, M. (2000), "Statistical analysis of thermal actions for concrete bridge design", *Structural Engineering International: Journal of the International Association for Bridge and Structural Engineering (IABSE)*, **10**(1), 33-38.

Tanker Fire Destroys Part of MacArthur Maze 2 Freeways Closed Near Bay Bridge, San Francisco Chronicle (2007), http://www.sfgate.com/cgi-bin/article.cgi?f=/c/a/2007/04/29/BAGVOPHQU46.DTL